Vision Research 51 (2011) 280–287

Contents lists available at ScienceDirect

Vision Research

journal homepage: www.elsevier.com/locate/visres

Visual responses in the lateral geniculate evoked by Cx36-independent rod pathways

Timothy M. Brown [a,*], Annette E. Allen [a], Jonathan Wynne [a], David L. Paul [b], Hugh D. Piggins [a], Robert J. Lucas [a]

[a] Faculty of Life Sciences, University of Manchester, Manchester, UK
[b] Dept. of Neurobiology, Harvard Medical School, 220 Longwood Ave., Boston, MA 02115, USA

ARTICLE INFO

Article history:
Received 11 June 2010
Received in revised form 9 August 2010
Available online 13 August 2010

Keywords:
Mouse
Scotopic
Melanopsin
Electroretinogram
Connexin

ABSTRACT

Emerging evidence indicates rods can communicate with retinal ganglion cells (RGCs) via pathways that do not involve gap-junctions. Here we investigated the significance of such pathways for central visual responses, using mice lacking a key gap junction protein ($Cx36^{-/-}$) and carrying a mutation that disrupts cone phototransduction ($Gnat2^{cpfl3}$). Electrophysiological recordings spanning the lateral geniculate revealed rod-mediated ON and OFF visual responses in virtually every cell from all major anatomical sub-compartments of this nucleus. Hence, we demonstrate that one or more classes of RGC receive input from Cx36-independent rod pathways and drive extensive ON and OFF responses across the visual thalamus.

1. Introduction

Rod bipolar cells are thought not to contact retinal ganglion cells (RGCs) directly, forcing rod signals to take a more circuitous route to reach these output neurons (Bloomfield & Dacheux, 2001; Sharpe & Stockman, 1999). Indeed, established views are that rods co-opt cone circuitry to communicate to the brain via two pathways with different sensitivities. The primary, highest sensitivity, rod pathway involves an excitatory chemical synapse between rod bipolar cells and AII amacrine cells which in turn couple to ON cone bipolar cells via gap junctions. A secondary, lower sensitivity pathway, involves gap junction connections between rods and cones themselves (Völgyi, Deans, Paul, & Bloomfield, 2004).

A critical component of both of these canonical rod pathways is gap-junction communication. These direct electrical connections between cells are formed by proteins of the connexin (Cx) family, of which Cx36 is particularly widely expressed in the mammalian retina. Cells expressing this protein include photoreceptors, cone bipolars and AII amacrine cells and, at least for these latter two retinal neurons, their coupling is dependent on its expression (Deans, Völgyi, Goodenough, Bloomfield, & Paul, 2002; Feigenspan, Teubner, Willecke, & Weiler, 2001; Mills, O'Brien, Li, O'Brien, & Massey, 2001). Moreover, consistent with the architecture of the established rod pathways, ON RGCs in $Cx36^{-/-}$ mice appear to completely lack rod-mediated signals (Deans et al., 2002).

However, over the past 10 years evidence has emerged for the existence of rod pathways that do not rely on gap-junctions. Hence, it is now known that some rods contact OFF cone bipolar cells directly (Hack, Peichl, & Brandstätter, 1999; Tsukamoto, Morigiwa, Ueda, & Sterling, 2001) and OFF RGCs in $Cx36^{-/-}$ mice receive rod signals (Völgyi et al., 2004). Even more recently, anatomical and functional evidence has emerged for synapses between rods and ON cone bipolar cells (Abd-El-Barr et al., 2009; Pang et al., 2010; Tsukamoto et al., 2007). While these data call into question received wisdom regarding the functional organization of the retina, the reported lack of rod ON signals in $Cx36^{-/-}$ RGCs raises the possibility that any such gap-junction independent rod pathway only impacts on relatively rare ganglion cell classes and/or is of relatively minor significance for central visual responses.

It is thus important to determine which, if any, RGCs receive input from these novel rod pathways. Several lines of evidence led us to suspect that intrinsically photosensitive, melanopsin expressing, retinal ganglion cells (mRGCs; reviewed in Bailes & Lucas, 2010), might receive input from 'atypical' rod pathways that did not rely on gap-junction communication; (1) through mRGCs (Göz et al., 2008; Güler et al., 2008; Hatori et al., 2008), rods drive mouse circadian response to light across a broad (>5 log unit) range which appears to involve multiple rod pathways with different sensitivities (Lall et al., 2010), (2) direct contacts between rod bipolar cells and mRGCs have been previously reported (Østergaard, Hannibal, & Fahrenkrug, 2007) and (3) these cells are rare (~2% of the total

* Corresponding author. Tel.: +44 161 2755050.
E-mail address: timothy.brown@manchester.ac.uk (T.M. Brown).

0042-6989/$ - see front matter © 2010 Elsevier Ltd. All rights reserved.
doi:10.1016/j.visres.2010.08.010

ganglion cell population; Baver, Pickard, Sollars, & Pickard, 2008; Hatori et al., 2008) and could easily have escaped detection in the original characterization of *Cx36*$^{-/-}$ mice.

To investigate the role of Cx36-independent rod pathways in mRGC-mediated responses we utilized *Cx36*$^{-/-}$;*Gnat2*^{cpfl3} mice. In addition to their lack of Cx36, these animals bear a mutation in the cone-specific transducin α-subunit which renders cones dysfunctional (Chang et al., 2006). Electroretinography (ERG) confirmed that ON bipolar cell responses in these animals were equivalent to wildtype for dim flashes but deficient with brighter flashes in the photopic range, consistent with a loss of cone function. We then went onto record light responses directly from the intergeniculate leaflet (IGL) and surrounding lateral geniculate nuclei (LGN) in these mice, a major target of mRGCs (Ecker et al., 2010). Surprisingly, we found responses to brief light increments and decrements in virtually all LGN neurons. These responses appeared at relatively low light levels and saturated in the low photopic range, consistent with a rod origin. Many of these cells also exhibited sustained responses characteristic of melanopsin phototransduction suggesting that Cx36-independent rod signals may indeed be routed by mRGCs. By contrast, a substantial proportion (~40%) of the cells from which we recorded these rod signals showed no evidence of melanopsin input indicating at least one (presumably rare) class of conventional RGC receives rod ON signals in the absence of Cx36. In summary these data add to the weight of evidence for tertiary rod ON and OFF pathways in the mammalian retina and suggest their influence on central visual targets is widespread.

2. Methods

2.1. Animals

All animal care was in accordance with institutional and Home Office (UK) regulations and the UK Animals Scientific Procedures, Act 1986. Animals were kept in a 12-h dark/light cycle environment at a temperature of 22 °C with food and water ad libitum.

2.2. Electroretinography

2.2.1. Recording methodology

ERG responses were compared in *Cx36*$^{-/-}$;*Gnat2*^{cpfl3}, *Gnat1*$^{-/-}$;*Gnat2*^{cpfl3} and wild-type mice (aged 60–100 days). Experimentation was performed under dim red light (<2.4 $\log_{10}$ nW/cm^2, >650 nm), and mice were long-term dark adapted (>12 h) prior to recording. Mice were initially anaesthetized with intraperitoneal ketamine (70 mg/kg) and xylazine (7 mg/kg), which was maintained with an injection of subcutaneous ketamine (72 mg/ml) and xylazine (5 mg/ml).

Pupil dilation was achieved through application of mydriatics (tropicamide, 1%, and phenylephrine, 2.5%; Chauvin Pharmaceuticals, Essex, UK) to each eye. Hypromellose solution (0.5%; Alcon Laboratories Ltd., Herts, UK) was also applied to each eye to retain corneal moisture and to provide sufficient adherence of a contact lens electrode to the corneal surface. A silver wire bite bar provided head support and acted as a ground, and a needle reference electrode (Ambu® Neuroline) was inserted approximately 5 mm from the base of contralateral eye, sufficiently distal to exclude signal interference. Electrodes were connected to a Windows PC via a signal conditioner (Model 1902 Mark III, CED, Cambridge, UK) which differentially amplified (3000×) and filtered (band-pass filter cut-off 0.5–200 Hz) the signal, and a digitizer (Model 1401, CED). Throughout experimentation, core body temperature was maintained at ~37 °C via a custom-made hose coil connected to a water source at constant temperature. For 10 min prior to first recordings, electrode stability was monitored; electrodes displaying any baseline instability were rejected.

2.2.2. Scotopic ERGs

A xenon arc source (Cairn Research Ltd., Kent, UK) connected to a ganzfeld sphere provided white light flashes of equal intensity across the retina. To investigate the irradiance-response relationship of scotopic ERGs, light intensity was increased in a logarithmic scale using ND filters (Edmund Optics, York, UK) to provide corneal irradiances in the range of −4.8–3.2 $\log_{10}$ μW/cm. Light measurements were performed using a calibrated optical power meter (Macam Photometrics, Livingston, UK) and spectrophotometer (Ocean Optics, FL, USA). Calculated spectra were corrected according to photon energy and summed to determine the total photon flux at these intensities (which ranged between 4.6×10^8 and 4.6×10^{14} photons/cm^2/s). A series of 15 ms flashes were applied using an electrically controlled mechanical shutter (Cairn Research Ltd.). The inter-stimulus interval ranged from 1500 ms at dimmest intensities to 30 s at brightest intensities. The number of stimuli was reduced from 30 to 6 at increasing intensities, and an average trace was generated from recordings at each intensity. In addition, to assess the residual cone activity retained in young adult *Gnat2*^{cpfl3} mice, ERG responses of *Gnat1*$^{-/-}$;*Gnat2*^{cpfl3} mice were compared in response to white, 458 nm and 580 nm light flashes (10 nm bandwidth; 5.4×10^{12} and 1.6×10^{13} photons/cm^2/s respectively).

2.2.3. Photopic ERGs

Continuous bright white flashes (Grass Model PS33 Photic Stimulator, Astro-Med, Inc., RI, USA; fitted with a 400 nm high pass filter; 10 μs duration; peak corneal irradiance 3.3 $\log_{10}$ μW/cm^2) were applied at a frequency of 1.3 Hz against a rod-saturating, uniform white background light (metal halide source; 2.8 $\log_{10}$ μW/cm^2). This was maintained over a period of 20 min, and ERGs were recorded following each light pulse. Recordings were then grouped into sets of 25, and an average trace was generated for each set.

2.2.4. Data analysis

The amplitude of the a-wave (from the stable baseline prior to stimulus onset, to a-wave peak) and the b-wave (from a-wave peak to b-wave peak) were recorded for each dataset. Sigmoidal curves were fitted to all datasets ($y = V_{min} + (V_{max} - V_{min})/(1 + 10\text{^}((V_{50} - x)/\text{Slope}))$) using GraphPad Prism v.4 (GraphPad Software Inc., CA, USA). To compare datasets, *F*-tests were used to determine whether the best-fit parameters in the above relation differed significantly, i.e. whether curves were statistically distinguishable ($P < 0.05$).

2.3. In vivo neurophysiology

2.3.1. Surgical procedures

Adult male mice (80–120 days) were anaesthetized by i.p. injection of 30% (w/v) urethane (1.7 g/kg; Sigma, Dorset, UK) and placed in a stereotaxic apparatus (SR-15M; Narishige International Ltd., London, UK). Additional top up doses of anaesthetic (0.2 g/kg) were applied as required. Throughout the experiment the animal's temperature was maintained at 37 °C with a homeothermic blanket (Harvard Apparatus, Kent, UK). The skull surface was exposed and a small hole (~1 mm diam.) drilled 2.5 mm posterior and 2.3 mm lateral to the bregma. The pupil, contralateral to the craniotomy, was dilated with topical application of 1% (w/v) atropine sulphate (Sigma) and the cornea kept moist with mineral oil. A recording probe (A4X8-5 mm-50-200-413; Neuronexus, MI, USA) consisting of four shanks (spaced 200 μm), each with eight recordings sites (spaced 50 μm) was then positioned centrally on the exposed skull surface, perpendicular to the midline, and lowered to a

depth of 2.8–3.2 mm using a fluid filled micromanipulator (MO-10; Narishige).

2.3.2. Recording methodology

Once the recording probe was in position the recording chamber was covered with darkroom blackout material (Nova Darkroom, Warwick, UK) and the room lights dimmed. Under these conditions background photon flux within the recording chamber was below the limit of our detectors. Mice were dark adapted for 1 h, which also allowed neuronal activity to stabilize after probe insertion/repositioning, after which we began recording. Neural signals were acquired using a Recorder64 system (Plexon, TX, USA). Signals were amplified 3000×, highpass filtered at 300 Hz and digitized at 40 kHz. Multiunit activity (spikes with amplitudes >50 μV) were saved as timestamped waveforms and analyzed offline (see below). Light stimuli were delivered by a custom built LED based light source (Cairn Research Ltd.) which consisted of independently controlled blue and red LEDs (λ_{max}: 460 and 655 nm respectively) with appropriate band-pass filters (half peak width: ±10 nm). The light passed through a filter wheel with various neutral density filters and was focused onto a 5 mm diameter piece of opal diffusing glass (Edmund Optics Inc., UK) positioned 3 mm from the eye contralateral to the recording probe. LED intensity and filter wheel position were controlled by a PC running LabView 8.6 (National instruments). Light measurements were performed using a calibrated spectrophotometer and optical power meter as described above. Unattenuated intensities were 6.8×10^{15} and 3.5×10^{15} photons/cm^2/s for the blue and red stimuli respectively. Based the calculated spectra and visual pigment templates described by Govardovskii, Fyhrquist, Reuter, Kuzmin, and Donner (2000) these equate to rod fluxes of 5.1×10^{15} and 1.6×10^{12} and melanopsin fluxes of 6.2×10^{15} and 2.1×10^{11} photons/cm^2/s respectively.

Intensity response relationships spanning a 7 log unit range were initially calculated for blue and red light applied for 2 s with an inter-stimulus interval of 18 s. At each intensity, starting at the lowest (as corrected for effective rod stimulation) 20 trials were completed before increasing the light intensity by a factor of 10. After completion of a full irradiance-response relationship, three of the mice used were dark adapted for 1 h before determining a responses to 30 s 460 nm pulses in the photopic range (inter-stimulus interval of 90 s; four trials at each intensity), a stimulus designed to robustly activate mRGCs.

2.3.3. Histological analysis

For each experiment the location of the probe was verified histologically. Before recording the electrode was immersed in fluorescent dye (Cell Tracker CM-DiI; Invitrogen Ltd. Paisley, UK) and at the end of the experiment the mouse was perfused transcardially with 0.1 M phosphate buffered saline followed by 4% paraformaldehyde. The brain was removed, postfixed overnight, cryoproteced with 30% sucrose then sectioned at 100 μm on a freezing sledge microtome. For detection of DiI fluorescence, sections were mounted with Vectashield (Vectorlaboratories Ltd. Peterborough, UK), coverslipped and visualized using an Olympus BX51 with appropriate filter sets. Sections were scaled to account for shrinkage using the distance between electrode tracks and aligned with the corresponding mouse atlas sections (Paxinos & Franklin, 2001) to estimate the stereotaxic coordinates of each recording site.

2.3.4. Data analysis

Multichannel, multiunit recordings were analyzed in Offline Sorter (Plexon). After removing artifacts we used principal component based sorting to discriminate single units, identifiable as a distinct cluster of spikes in principal component space with a clear refractory period in their interspike interval distribution. In most cases there was a single distinct unit at each recording site (total 95 units from 128 recording sites). Following spike sorting data were exported to Neuroexplorer (Nex technologies, MA, USA) and MATLAB R2007a (The Mathworks Inc., MA, USA) for construction of peristimulus histograms and further analysis. Light responsive units were identified as those where the peristimulus average showed a clear peak (or trough) that exceeded the 99% confidence limits estimated from a Poisson distribution derived from the peristimulus spike counts. Intensity response relationships for 460 nm and 655 nm light pulses (with intensities corrected for rod or melanopsin stimulation as described above) were fit with sigmoid functions using GraphPad Prism as described above for ERG recordings. 'Sustained' light responsive cells were defined as those for which the spike rate 1–2 s following the onset of our unattenuated 460 nm stimulus was significantly elevated relative to the spike rate 1 s before light onset (paired *t*-test of 20 trials, $P < 0.05$). The remaining cells were defined as 'transient'.

3. Results

We performed ERG recordings in four *Cx36*$^{-/-}$;*Gnat2*^{cpfl3} mice and five wildtype animals (Fig. 1). Consistent with previous data from *Gnat2*^{cpfl3} mice (Chang et al., 2006) and the view that Cx36 is not an element of rod to rod bipolar cell communication, b-wave responses to dim flashes in *Cx36*$^{-/-}$;*Gnat2*^{cpfl3} mice exhibited essentially identical amplitude and sensitivity to wild-type mice. However, at intensities above 4.6×10^{10} photons/cm^2/s b-waves in the *Cx36*$^{-/-}$;*Gnat2*^{cpfl3} mice were substantially reduced in amplitude relative to wildtype. Indeed *F*-tests indicated that, while responses of the two genotypes at the lower intensity range could be fit by a single sigmoidal function ($F = 0.37$, $P > 0.05$), responses at higher intensities were better explained by separate functions ($F = 6.91$, $P < 0.001$). The point at which these intensity response functions diverge (above 2.2×10^{10} photons/cm^2/s when corrected according to the sensitivity of mouse cones) corresponds to the threshold for cone based responses in mice (Nathan et al., 2006; Pang et al., 2010). These data indicate that, while rod function appears normal in these *Cx36*$^{-/-}$;*Gnat2*^{cpfl3} mice, cone responses are severely curtailed.

The original report on *Gnat2*^{cpfl3} mice indicated that they exhibit a small photopic ERG that is lost between 2 and 9 months of age (Chang et al., 2006). In agreement with the findings of that earlier study, under rod-saturating background lights, the *Cx36*$^{-/-}$;*Gnat2*^{cpfl3} mice used in our study (2–3 months old) retained a flash ERG response (Fig. 1C). However, unlike responses in wild-type mice, this did not increase in magnitude over the course of 20 min light adaptation such that by the end of this epoch *Cx36*$^{-/-}$;*Gnat2*^{cpfl3} b-wave amplitude was only ~30% of wildtype levels (28 ± 10 vs. 102 ± 11 μV). To estimate the contribution of this residual cone activity in the *Gnat2*^{cpfl3} mutants under dark adapted conditions we also measured ERG responses in two *Gnat1*$^{-/-}$;*Gnat2*^{cpfl3} mice. In these animals, ablation of the rod-specific a transducin (*Gnat1*) abolishes scotopic responses at the retinal and behavioral level (Abd-El-Barr et al., 2009; Calvert et al., 2000; Nathan et al., 2006). In both individuals, bright white flashes from darkness (4.6×10^{14} photons/cm^2/s, 3.2 and 2.6×10^{14} photons/cm^2/s as corrected according to the sensitivity of rods and cones respectively) revealed a small (53 and 29 μV) b-wave (Fig. 1D). Lower intensities did not evoke measurable responses (not shown). Accordingly, narrowband blue (458 nm; 5.4×10^{12} photons/cm^2/s) or orange (580 nm; 5.4×10^{13} photons/cm^2/s) flashes also failed to evoke measurable responses in these *Gnat1*$^{-/-}$;*Gnat2*^{cpfl3} mice. On the basis of these recordings we conclude that, any responses in *Cx36*$^{-/-}$;*Gnat2*^{cpfl3} mice evoked by light intensities below 10^{13} photons/cm^2/s cannot be explained by their residual cone sensitivity.

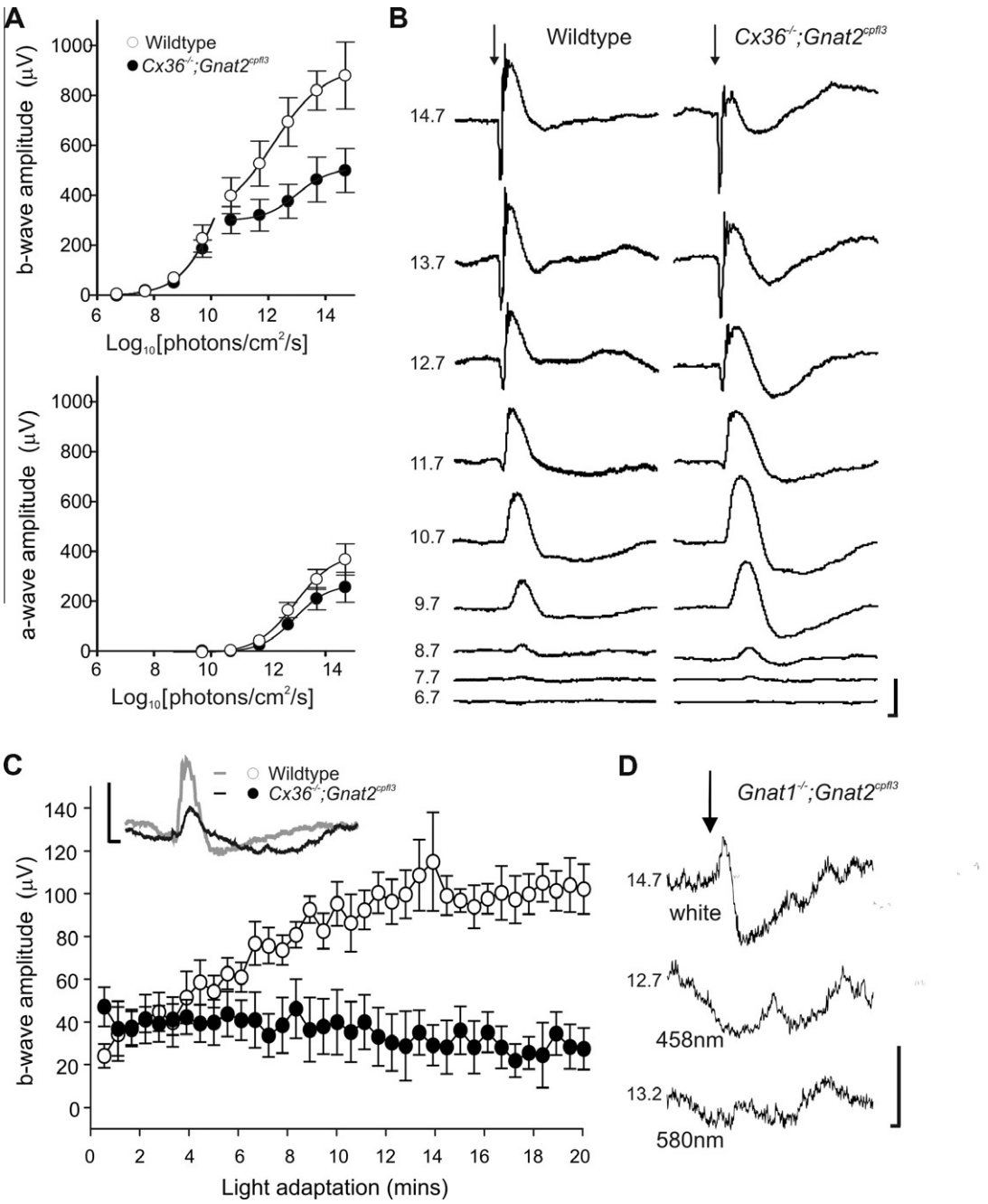

Fig. 1. Cone, but not rod, function is impaired in $Cx36^{-/-}$;$Gnat2^{cpfl3}$ mice. (A) Quantification and (B) representative traces of wildtype and $Cx36^{-/-}$;$Gnat2^{cpfl3}$ dark-adapted ERGs. (A) Comparison of a- and b-wave amplitudes from wild-type and $Cx36^{-/-}$;$Gnat2^{cpfl3}$ mice, data points represent mean ± SEM. b-Wave responses of the two genotypes below 10^{10} photons/cm^2/s could be fit by a single curve ($F = 0.37$, $P > 0.05$) while responses at higher intensities could not ($F = 6.91$, $P < 0.001$). a-Wave amplitudes of the two genotypes were also better fit by separate curves ($F = 3.25$, $P < 0.05$). (C) Quantification of photopic ERG responses in wild-type and $Cx36^{-/-}$;$Gnat2^{cpfl3}$ mice (inset shows representative examples). An attenuated, non-adapting, photopic ERG response is retained in $Cx36^{-/-}$;$Gnat2^{cpfl3}$ mice. (D) Average ERG responses of $Gnat1^{-/-}$/$Gnat2^{cpfl/cpfl}$ mice to white light, 458 nm and 580 nm light. No measurable ERG was present in response to flashes of 458 or 580 nm, while bright white light resulted in a small response (n = 2). Scale bars: *x*-axis = 50 ms *y*-axis = 200 μV in B or 100 μV in C and D. Numbers to left of trace in B and D represent $\log_{10}$[photons/cm^2/s].

To determine whether the intact rod responses in these mice were communicated via RGCs to the brain in the absence of Cx36 gap junctions, we recorded multichannel (32 ch.) multiunit activity from the IGL and surrounding LGN of four $Cx36^{-/-}$;$Gnat2^{cpfl3}$ mice (Fig. 2A; including the three mice used for our ERG studies) using a stimulus that was sub-threshold for the cone evoked ERG in $Gnat1^{-/-}$;$Gnat2^{cpfl3}$ mice (6.8×10^{11} photons/cm^2/s at 460 nm). These experiments revealed robust responses to light increments and decrements that spanned all regions of the LGN that we recorded from. Hence, ON and OFF responses reach the brain in the absence of Cx36 gap junctions and functioning cones.

Spike sorting of this multiunit spike data resolved 95 single units of which 63 exhibited clear light responses (Fig. 2B and C), with almost all the light un-response units (28/32) detected at recording sites lying outside the boundaries of the LGN. In addition, for another 17 recording sites located within the LGN we observed robust multiunit light responses but were unable to reliably isolate single unit activity. Based on the widespread thalamic light responses we observed in these experiments we reasoned that, whatever the pathway by which light information reaches LGN-projecting RGCs in $Cx36^{-/-}$;$Gnat2^{cpfl3}$ mice it appears to be fairly ubiquitous. Indeed from the single unit responses, we identified

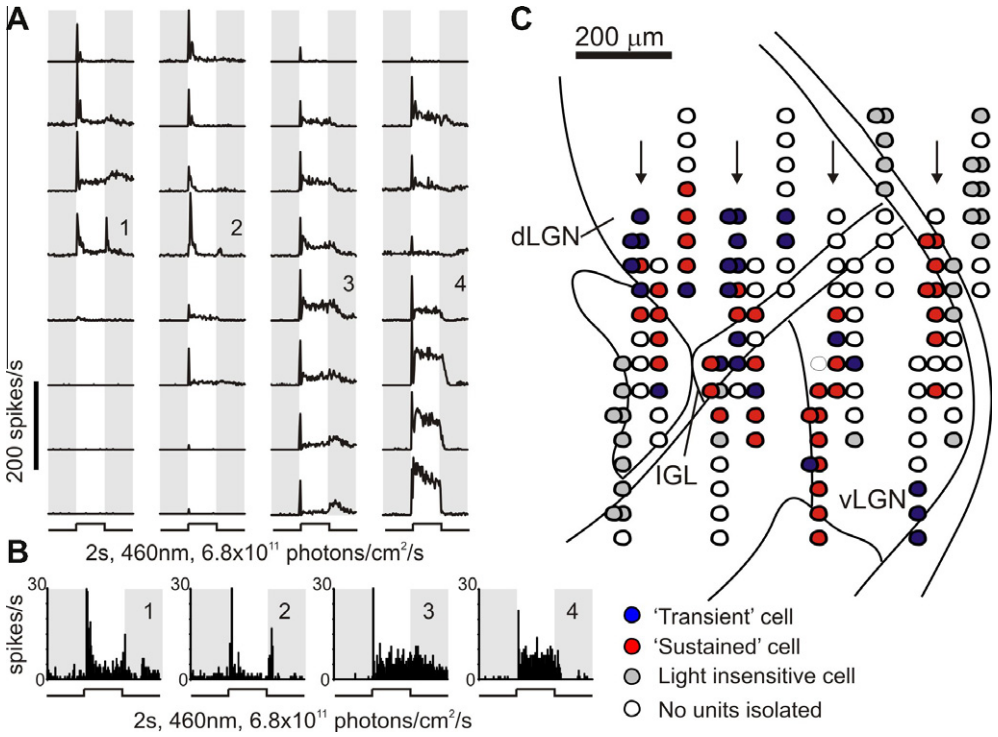

Fig. 2. Thalamic light responses in *Cx36*$^{-/-}$;*Gnat2*^{cpfl3} mice. (A) Multiunit spiking response to 2 s (460 nm) light steps, detected using a 32 ch. electrode placed in the central LGN of a *Cx36*$^{-/-}$;*Gnat2*^{cpfl3} mouse. Traces represent average of 20 responses, shaded areas represent darkness. (B) Examples of light responsive single units discriminated from the multiunit recordings at numbered sites in (A). Light responsive units could be categorized into two classes (based on responses to higher intensities; see Section 2); 'transient' cells which showed brief increase in spike rate at light on and off (B1,2) and 'sustained cells (B3,4) which maintained elevated discharge rates throughout the light stimulus. (C) Projected anatomical locations of single units detected from recordings in four *Cx36*$^{-/-}$;*Gnat2*^{cpfl3} mice. Overlapping symbols indicate recording sites where we could isolate two distinct units. Cells that lacked clear light responses were almost exclusively found outside the LGN. Arrows indicate the regions spanned by recording sites in (A). Note that at some sites we were unable to isolate a clear single unit despite robust multiunit light responses. d/vLGN = dorsal/ventral lateral geniculate, IGL = intergeniculate leaflet.

the distinct 'sustained' and 'transient' types of light responsive cell that have been observed previously in various species (Cleland, Dubin, & Levick, 1971; Grubb & Thompson, 2003; Harrington & Rusak, 1989; Van Hooser, Heimel, & Nelson, 2003). These could be distinguished on the basis of the persistence of their light response (see Section 2). Both showed robust, phasic, elevations in spike rate at light on and somewhat smaller excitatory responses following termination of the light stimulus. However, whereas in one cell type ('transient'; $n = 25$) these responses quickly returned to near baseline, in other cells these responses only partially decayed ('sustained'; $n = 38$).

To fully define the sensitivity and dynamic range over which cells in *Cx36*$^{-/-}$;*Gnat2*^{cpfl3} mice responded to light we described intensity response relationships to 2 s light steps at 460 and 655 nm (Fig. 3). For both 'sustained' and 'transient' cells we quantified the magnitude of the phasic ON (0–500 ms following light on), tonic ON (1–2 s following light on) and phasic OFF (0–1 s after light off) excitations relative to baseline firing. Individual LGN cells reliably responded to 655 nm light pulses at or below 3.8×10^{10} photons/cm^2/s, corresponding to an effective photon flux for rods of 1.6×10^7 photons/cm^2/s (see Section 2), close to the threshold for scotoptic vision in mice and ~3 orders of magnitude more sensitive than the threshold for cone vision (Nathan et al., 2006). These responses built up over the scotopic range and, consistent with disrupted cone function in these *Cx36*$^{-/-}$;*Gnat2*^{cpfl3} mice, reached maximal values below 10^{12} rod stimulating photons/cm^2/s. Indeed, the spectral sensitivity of rods could account for all almost all the responses we observed to these brief light steps over this range of intensities. Hence, when we corrected the photon flux of the red and blue lights according to their relative stimulation of rods, sigmoidal functions fit to the intensity responses relationships for the two wavelengths were statistically indistinguishable (*F*-tests; 'transient' ON: $F = 1.09$; tonic: n/a; OFF: $F = 0.022$; 'sustained' ON: 3.47; tonic: 1.98; OFF: 0.812; all $P > 0.05$). By contrast, when intensities were corrected according to the sensitivity of melanopsin, responses to each wavelength were better fit by separate curves (*F*-tests; 'transient' ON: $F = 4.76$; tonic: n/a; OFF: $F = 6.722$; 'sustained' ON: 15.1; tonic: 5.05; OFF: 5.99; all $P < 0.05$).

However, in the 'sustained' but not 'transient' population we consistently observed tonic, supramaximal, responses to 460 nm light ~3 orders of magnitude brighter than the saturation point for all other responses (Fig. 3B). We suspected that these responses reflected the recruitment for melanopsin phototransduction. The more ventral components of the LGN targeted by our electrodes (the IGL and vLGN) are well known to receive dense input from mRGCs (Hattar et al., 2006) and there is new evidence that this is also true of the dorsal LGN (Ecker et al., 2010). Indeed, we have functionally characterized the 'sustained' cells found in the LGN of other mouse strains and found melanopsin input to be a defining feature of this response type wherever it is encountered (Brown, Gigg, Piggins, & Lucas, 2010). Consistent with these findings and existing data suggesting that sustained signals from the outer retina may be exclusively routed via mRGCs (Wong, Dunn, Graham, & Berson, 2007), *Cx36*$^{-/-}$;*Gnat2*^{cpfl3} cells that showed this evidence of melanopsin input at high irradiances also exhibited considerably more sustained responses at dim-moderate irradiances (subthreshold for melanopsin activation) than did 'transient' cells.

To further confirm our characterization of 'sustained' and 'transient' cells and to better ascertain whether any of these *Cx36*$^{-/-}$;*Gnat2*^{cpfl3} cells did indeed display responses characteristic of mRGC input, we utilized long duration (30 s) bright blue light

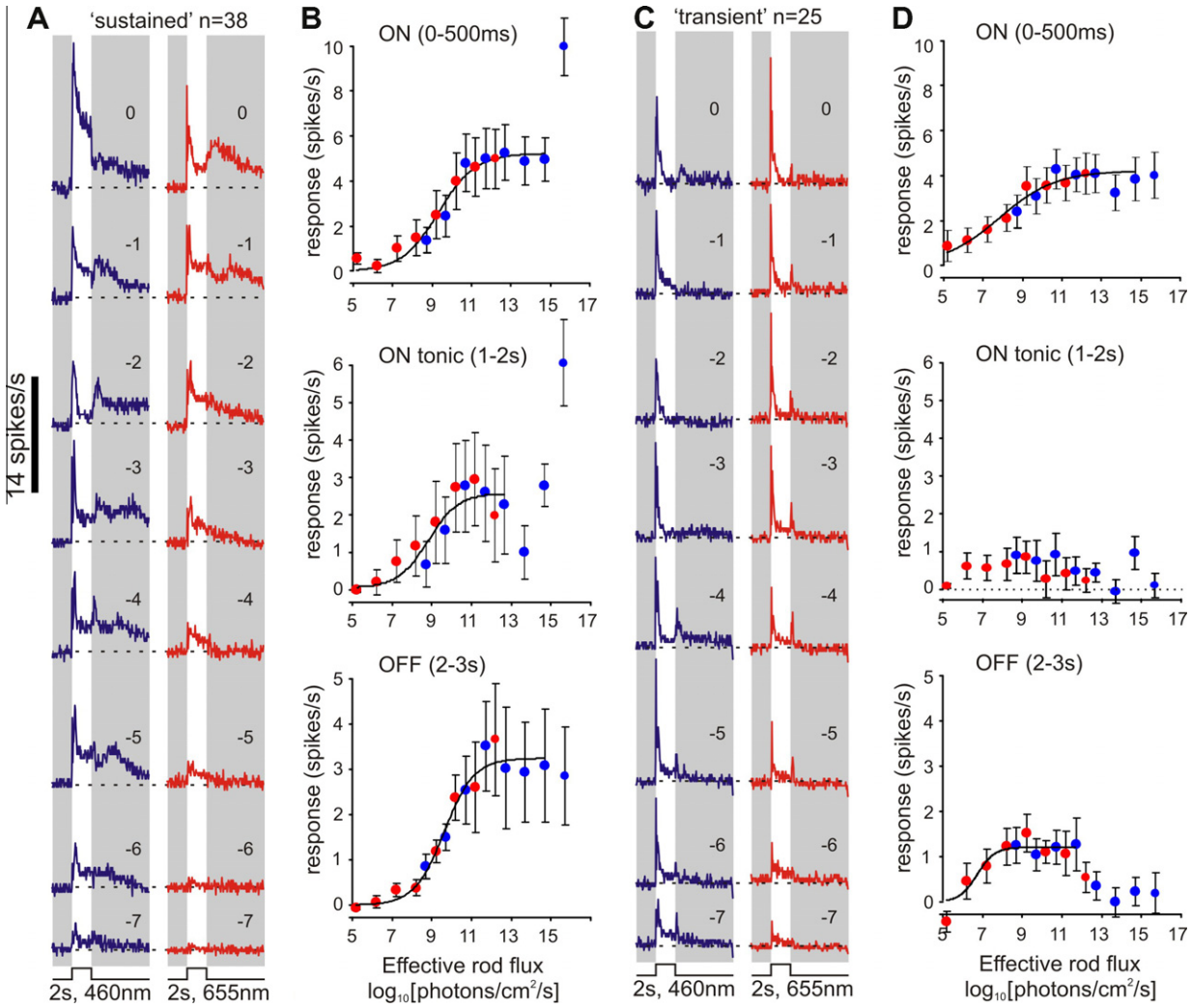

Fig. 3. Rods signal to the brain in the absence of Cx36 gap-junctions. (A and C) average response waveforms (bin size 50 ms) of 'sustained' (A) and 'transient' (B) LGN neurons to 460 nm and 655 nm light steps (2 s duration) of increasing intensity (bottom to top). Numbers above traces represent $\log_{10}$[intensity] relative to the unattenuated intensities: 6.8×10^{15} and 3.6×10^{15} photons/cm^2/s for the 460 nm and 655 nm stimuli respectively. (B and D) Quantification of ON, tonic and OFF components of the response of 'sustained' (B) and 'transient' (D) LGN neurons. Data points represent the mean(±SEM) response of all cells, calculated as the mean change in spike rate during the first 500 ms following light on (top panels), 1–2 s following light on (middle panels) or the first 1 s following light off (bottom panels). Intensities were corrected according to the sensitivity of rods to the 460 nm and 655 nm lights and fit with sigmoid functions as described in Section 2. Tonic responses of 'transient' cells were not well fit by such functions. For all other parameters, blue/red responses were better fit by a common function than two separate curves when corrected in this way (*F*-tests, all $P > 0.05$) but not when corrected according to the sensitivity of melanopsin ($P < 0.05$).

steps. Whereas, 'transient' cells showed little response under these conditions, 'sustained' cells exhibited robust and prolonged increases in spike rate that built up over the photopic range (Fig. 4). Consistent with our extensive data in other strains that the 'sustained' cells receive melanopsin input (Brown et al., 2010), these responses nicely matched the well established sensitivity and kinetics of mRGC intrinsic photoresponses (Berson, Dunn, & Takao, 2002; Dacey et al., 2005; Tu et al., 2005; Wong et al., 2007).

4. Discussion

Here we demonstrate that rod signals can drive an array of responses in the brain in the absence of Cx36 containing gap junctions. These include transient 'On' and 'Off' excitation as well as sustained activation under extended light exposure. Rod-mediated responses have previously been observed in *Cx36*$^{-/-}$ OFF RGCs (Völgyi et al., 2004), but not other ganglion cell types. These data, to our knowledge, constitute the first demonstration that such an array of rod-dependent information can arise from Cx36-independent visual pathways. Since such signals have not previously been observed at the RGC level but appear widespread in the brain, we argue that such tertiary rod pathway(s) are selectively utilized by one or more rare classes of ganglion cells capable of relatively wide-ranging influence.

The sensitivity and dynamic range of the central responses we reveal here, which emerged by 10^7 photons/cm^2/s and saturated below 10^{12} photons/cm^2/s, are very similar to those previously reported for rod signals in a subtype of cone ON bipolar cells in *Cx36*$^{-/-}$ (and wild-type) mice (Pang et al., 2010). By contrast, light responses in AII amacrine cells, which require Cx36 to couple to downstream retinal circuitry are ~2 orders of magnitude more sensitive (Deans et al., 2002; Wu, Gao, & Pang, 2004). Based on recent data indicating that rods form chemical synapses with subtypes of cone ON and OFF bipolar cells (Tsukamoto et al., 2001, 2007), we suggest that our data reflect rod signals traveling via these tertiary rod pathways that do not involve gap junctions.

The original description of *Gnat2*^{cpfl3} mice indicated that these animals retain normal scotopic responses and a small (~25% of normal) photopic ERC that is lost between 2 and 9 months of age

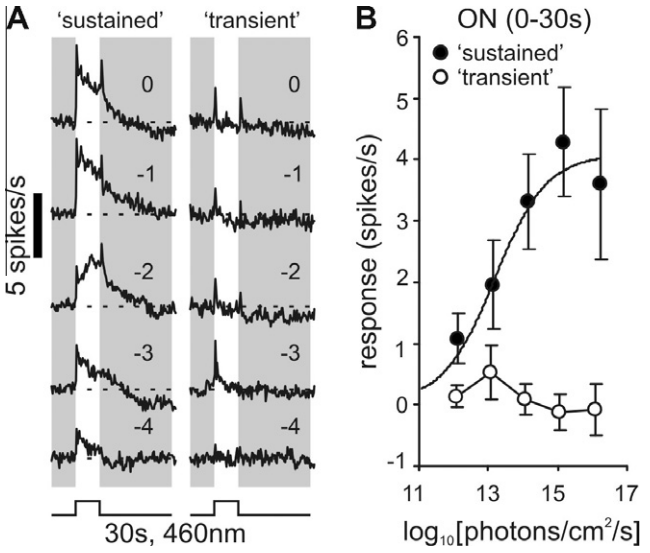

Fig. 4. Bright light responses in 'sustained' LGN neurons consistent with melanopsin input. (A) average response waveforms (bin size 1 s) of 'sustained' (left; $n = 30$) and 'transient' (right: $n = 24$) LGN neurons to 460 nm light steps (30 s duration) of increasing intensity (bottom to top). Numbers above traces represent $\log_{10}$[intensity] relative to the unattenuated intensity (6.8×10^{15} photons/cm^2/s). (B) Quantification of the response of 'sustained' and 'transient' LGN neurons. Data points represent the mean(±SEM) response of all cells, calculated as the mean change in spike rate during the 30 s that the light was on. 'Sustained' but not 'transient' cells showed robust long lasting responses that built up over the mid-high photopic range, characteristic of melanopsin responses.

(Chang et al., 2006). Consistent with these data, we found that *Cx36*$^{-/-}$;*Gnat2*^{cpfl3} mice (2–3 months old) exhibited normal responses to dim, but not bright, flashes and a small ERG response under photopic (rod-saturating) conditions that did not adapt over time. In sum, these data confirm that while the *Gnat2* mutation dramatically reduces cone responses they are not completely abolished.

One possibility to address therefore is that the LGN responses we observe in *Cx36*$^{-/-}$;*Gnat2*^{cpfl3} mice reflect residual cone activity. We consider this most unlikely. Using *Gnat1*$^{-/-}$;*Gnat2*^{cpfl3} mice we estimate the threshold for the *Gnat2*^{cpfl3}-resistant cone ERG to be >10^{13} photons/cm^2/s. It is formally possible that the sensitivity of LGN neurons to the residual cone signals in *Gnat2*^{cpfl3} strains could be somewhat higher than this. However, while integrating input from many bipolar cells can increase sensitivity of RGC spike responses by an order of magnitude (Wu et al., 2004), 50% or less of these RGC input spikes trigger an LGN output spike (Kaplan & Shapley, 1984). As LGN cells generally receive input from 1 (and at most 2) RGCs (Chen & Regehr, 2000; Jaubert-Miazza et al., 2005), it seems most unlikely that the sensitivity of *Gnat2*^{cpfl3} LGN cells to cone inputs could exceed our estimates based upon the ERG (which reports activity across the entire population of bipolar cell population) by more than 1 log unit. By contrast, the threshold for LGN responses in *Cx36*$^{-/-}$;*Gnat2*^{cpfl3} mice at 1.6×10^7 rod-corrected photons/cm^2/s while very similar to that for ERG responses in this genotype (2.1×10^7 rod-corrected photons/cm^2/s) is at least six orders of magnitude lower than that for *Gnat2*^{cpfl3}-resistant cone ERG, and indeed ~3 orders of magnitude lower than the threshold for cone based vision in mice (Nathan et al., 2006; Pang et al., 2010).

A large proportion (~60%) of the cells in which we recorded these rod signals also showed sustained responses to bright light. These responses could partly involve the residual cone activity associated with the *Gnat2*^{cpfl3} mutation. However, we feel they at least mainly arise through the intrinsic photosensitivity of mRGCs. The IGL and vLGN and dLGN are densely innervated by mRGCs (Ecker et al., 2010). Moreover, the responses we recorded matched the documented sensitivity and kinetics of melanopsin phototransduction (Berson et al., 2002; Dacey et al., 2005; Tu et al., 2005; Wong et al., 2007). Indeed, mRGC input defines the population of 'sustained' LGN neurons, which are found in high numbers through the LGN in other mouse strains (Brown et al., 2010). Our data are therefore compatible with the notion that cone bipolar cells receiving chemical synapses from rods communicate with mRGCs and/or that rod bipolar cells communicate directly with mRGCs (Østergaard et al., 2007). If this is the case it is perhaps not surprising that these gap-junction independent rod signals escaped detection in the original studies of ON RGCs in *Cx36*$^{-/-}$ mice (Deans et al., 2002; Völgyi et al., 2004), since mRGCs constitute only ~2% of the total ganglion cell population (Baver et al., 2008; Hatori et al., 2008).

Rod signals were also apparent in the ~40% of neurons that showed 'transient' responses to light. That is, the population that appears to lack mRGC input. In this regard, it seems clear that not all rod signals could come via mRGCs in this model. Rather at least one class of conventional, non-photoreceptive, RGC appears to receive input from Cx36-independent rod pathways. Indeed, it is formally possible that this non-mRGC ganglion cell also provides the rod signal for cells with the 'sustained' response phenotype. Some LGN neurons may receive input from more than one RGC (Chen & Regehr, 2000; Jaubert-Miazza et al., 2005), allowing the possibility that separate ganglion cells contribute the Cx36-independent rod and melanopsin dependent components of the 'sustained' responses.

To summarise, our findings add to the weight of evidence for the existence of gap-junction independent rod pathways. Moreover, the sensory capabilities of such pathways appears fairly extensive, allowing for sustained and transient, ON and OFF, signals, just as in mice with an intact visual system (Grubb & Thompson, 2003). Future work will need to define exactly which populations of RGCs make use of these pathways but, based on our data, such an event cannot be peculiar to mRGCs but must also include at least one population of conventional RGC. In any case, whichever RGC populations do receive input from these tertiary rod pathways they are likely to be low in numbers but clearly can have a wide-ranging impact at the level of the LGN. While it remains to be determined whether the influence of *Cx36*-independent rod pathways is as extensive in wild-type mice as in the *Cx36*$^{-/-}$;*Gnat2*^{cpfl3} mice employed in this study our data suggest caution in assuming that *Cx36*$^{-/-}$ mice lack rod vision.

Acknowledgements

Cyrus Arman (USC Keck School of Medicine) kindly provided the initial breeding stock of *Cx36*$^{-/-}$;*Gnat2*^{cpfl3} mice. Funding was provided by the Wellcome trust UK (RJL and HDP); and the NIH (GM37751 and EY014127 to DLP).

References

Abd-El-Barr, M. M., Pennesi, M. E., Saszik, S. M., Barrow, A. J., Lem, J., Bramblett, D. E., et al. (2009). Genetic dissection of rod and cone pathways in the dark-adapted mouse retina. *Journal of Neurophysiology, 102*, 1945–1955.

Bailes, H. J., & Lucas, R. J. (2010). Melanopsin and inner retinal photoreception. *Cellular and Molecular Life Sciences, 67*, 99–111.

Baver, S. B., Pickard, G. E., Sollars, P. J., & Pickard, G. E. (2008). Two types of melanopsin retinal ganglion cell differentially innervate the hypothalamic suprachiasmatic nucleus and the olivary pretectal nucleus. *European Journal of Neuroscience, 27*, 1763–1770.

Berson, D. M., Dunn, F. A., & Takao, M. (2002). Phototransduction by retinal ganglion cells that set the circadian clock. *Science, 295*, 1070–1073.

Bloomfield, S. A., & Dacheux, R. F. (2001). Rod vision: Pathways and processing in the mammalian retina. *Progress in Retinal and Eye Research, 20*, 351–384.

Brown, T.M., Gigg, J., Piggins, H.D., & Lucas, R.J.L. (2010). Melanopsin-dependent activation of dorsal lateral geniculate neurons. ARVO annual meeting: 672.

Calvert, P. D., Krasnoperova, N. V., Lyubarsky, A. L., Isayama, T., Nicoló, M., Kosaras, B., et al. (2000). Phototransduction in transgenic mice after targeted deletion of

the rod transducin alpha -subunit. *Proceedings of the National Academy of Sciences USA, 97*, 13913–13918.
Chang, B., Dacey, M. S., Hawes, N. L., Hitchcock, P. F., Milam, A. H., Atmaca-Sonmez, P., et al. (2006). Cone photoreceptor function loss-3, a novel mouse model of achromatopsia due to a mutation in Gnat2. *Investigative Ophthalmology & Visual Science, 47*, 5017–5021.
Chen, C., & Regehr, W. G. (2000). Developmental remodeling of the retinogeniculate synapse. *Neuron, 28*, 955–966.
Cleland, B. G., Dubin, M. W., & Levick, W. R. (1971). Sustained and transient neurones in the cat's retina and lateral geniculate nucleus. *Journal of Physiology, 217*, 473–496.
Dacey, D. M., Liao, H. W., Peterson, B. B., Robinson, F. R., Smith, V. C., Pokorny, J., et al. (2005). Melanopsin-expressing ganglion cells in primate retina signal colour and irradiance and project to the LGN. *Nature, 433*, 749–754.
Deans, M. R., Völgyi, B., Goodenough, D. A., Bloomfield, S. A., & Paul, D. L. (2002). Connexin36 is essential for transmission of rod-mediated visual signals in the mammalian retina. *Neuron, 36*, 703–712.
Ecker, J. L., Dumitrescu, O. N., Wong, K. Y., Alam, N. M., Chen, S. K., LeGates, T., et al. (2010). Melanopsin-expressing retinal ganglion-cell photoreceptors: Cellular diversity and role in pattern vision. *Neuron, 67*, 49–60.
Feigenspan, A., Teubner, B., Willecke, K., & Weiler, R. (2001). Expression of neuronal connexin36 in AII amacrine cells of the mammalian retina. *Journal of Neuroscience, 21*, 230–239.
Govardovskii, V. I., Fyhrquist, N., Reuter, T., Kuzmin, D. G., & Donner, K. (2000). In search of the visual pigment template. *Visual Neuroscience, 17*, 509–528.
Göz, D., Studholme, K., Lappi, D. A., Rollag, M. D., Provencio, I., & Morin, L. P. (2008). Targeted destruction of photosensitive retinal ganglion cells with a saporin conjugate alters the effects of light on mouse circadian rhythms. *PLoS One, 3*, e3153.
Grubb, M. S., & Thompson, I. D. (2003). Quantitative characterization of visual response properties in the mouse dorsal lateral geniculate nucleus. *Journal of Neurophysiology, 90*, 3594–3607.
Güler, A. D., Ecker, J. L., Lall, G. S., Haq, S., Altimus, C. M., Liao, H. W., et al. (2008). Melanopsin cells are the principal conduits for rod-cone input to non-image-forming vision. *Nature, 453*, 102–105.
Hack, I., Peichl, L., & Brandstätter, J. H. (1999). An alternative pathway for rod signals in the rodent retina: rod photoreceptors, cone bipolar cells, and the localization of glutamate receptors. *Proceedings of the National Academy of Sciences USA, 96*, 14130–14135.
Harrington, M. E., & Rusak, B. (1989). Photic responses of geniculo-hypothalamic tract neurons in the Syrian hamster. *Visual Neuroscience, 2*, 367–375.
Hatori, M., Le, H., Vollmers, C., Keding, S. R., Tanaka, N., Buch, T., et al. (2008). Inducible ablation of melanopsin-expressing retinal ganglion cells reveals their central role in non-image forming visual responses. *PLoS One, 3*, e2451.
Hattar, S., Kumar, M., Park, A., Tong, P., Tung, J., Yau, K. W., et al. (2006). Central projections of melanopsin-expressing retinal ganglion cells in the mouse. *Journal of Comparative Neurology, 497*, 326–349.
Jaubert-Miazza, L., Green, E., Lo, F. S., Bui, K., Mills, J., & Guido, W. (2005). Structural and functional composition of the developing retinogeniculate pathway in the mouse. *Visual Neuroscience, 22*, 661–676.
Kaplan, E., & Shapley, R. (1984). The origin of the S (slow) potential in the mammalian lateral geniculate nucleus. *Experimental Brain Research, 55*, 111–116.
Lall, G. S., Revell, V. L., Momiji, H., Al Enezi, J., Altimus, C. M., Güler, A. D., et al. (2010). Distinct contributions of rod, cone, and melanopsin photoreceptors to encoding irradiance. *Neuron, 66*, 417–429.
Mills, S. L., O'Brien, J. J., Li, W., O'Brien, J., & Massey, S. C. (2001). Rod pathways in the mammalian retina use connexin 36. *Journal of Comparative Neurology, 436*, 336–350.
Nathan, J., Reh, R., Ankoudinova, I., Ankoudinova, G., Chang, B., Heckenlively, J., et al. (2006). Scotopic and photopic visual thresholds and spatial and temporal discrimination evaluated by behavior of mice in a water maze. *Photochemistry & Photobiology, 82*, 1489–1494.
Østergaard, J., Hannibal, J., & Fahrenkrug, J. (2007). Synaptic contact between melanopsin-containing retinal ganglion cells and rod bipolar cells. *Investigative Ophthalmology and Visual Science, 48*, 3812–3820.
Pang, J. J., Gao, F., Lem, J., Bramblett, D. E., Paul, D. L., & Wu, S. M. (2010). Direct rod input to cone BCs and direct cone input to rod BCs challenge the traditional view of mammalian BC circuitry. *Proceedings of the National Academy of Sciences USA, 107*, 395–400.
Paxinos, G., & Franklin, K. B. J. (2001). *The mouse brain in stereotaxic coordinates:* (2nd ed.). San Diego: Academic press.
Sharpe, L. T., & Stockman, A. (1999). Rod pathways: the importance of seeing nothing. *Trends in Neuroscience, 22*, 497–504.
Tsukamoto, Y., Morigiwa, K., Ishii, M., Takao, M., Iwatsuki, K., Nakanishi, S., et al. (2007). A novel connection between rods and ON cone bipolar cells revealed by ectopic metabotropic glutamate receptor 7 (mGluR7) in mGluR6-deficient mouse retinas. *Journal of Neuroscience, 27*, 6261–6267.
Tsukamoto, Y., Morigiwa, K., Ueda, M., & Sterling, P. (2001). Microcircuits for night vision in mouse retina. *Journal of Neuroscience, 21*, 8616–8623.
Tu, D. C., Zhang, D., Demas, J., Slutsky, E. B., Provencio, I., Holy, T. E., et al. (2005). Physiologic diversity and development of intrinsically photosensitive retinal ganglion cells. *Neuron, 48*, 987–999.
Van Hooser, S. D., Heimel, J. A., & Nelson, S. B. (2003). Receptive field properties and laminar organization oflateral geniculate nucleus in the gray squirrel (*Sciurus carolinensis*). *Journal of Neurophysiology, 90*, 3398–3418.
Völgyi, B., Deans, M. R., Paul, D. L., & Bloomfield, S. A. (2004). Convergence and segregation of the multiple rod pathways in mammalian retina. *Journal of Neuroscience, 24*, 11182–11192.
Wong, K. Y., Dunn, F. A., Graham, D. M., & Berson, D. M. (2007). Synaptic influences on rat ganglion-cell photoreceptors. *Journal of Physiology, 582*, 279–296.
Wu, S. M., Gao, F., & Pang, J. J. (2004). Synaptic circuitry mediating light-evoked signals in dark-adapted mouse retina. *Vision Research, 44*, 3277–3288.